


## Research Paper

# Frequency and Voltage Stability of the Islanded Microgrid with Multi DC-BUS Based-Inverter using Droop Control

A.T. Alahmad, Alireza Saffarian<sup>\*</sup> , Seyyed Ghodrattollah Seifossadat<sup>†</sup> , and Seyed Saeedallah Mortazavi<sup>†</sup> 

Department of Electrical Engineering, Shahid Chamran University of Ahvaz, Ahvaz, Iran

**Abstract**— The widespread adoption of microgrids in electric power systems has brought numerous advantages such as decentralized control, reliability, cost-effectiveness, and environmental benefits. However, one of the most critical challenges faced by islanded microgrids is ensuring frequency and voltage stability. This paper addresses these stability issues that arise when microgrids operate independently, disconnected from the main network through the point of common coupling (PCC). These microgrids rely on renewable resources like photovoltaic (PV) systems, wind turbines, and energy storage systems, which often require DC to AC conversion through inverters to simulate synchronous generators. To overcome the frequency and voltage stability challenges, this research utilizes the droop control technique to regulate the active and reactive power of distribution generators (DGs). The droop control technique is implemented and simulated using MATLAB software, specifically employing a multi-DC bus-based inverter. The simulation results demonstrate that the DGs successfully supply the required total power to meet load demands while maintaining frequency and voltage stability. Through the droop control technique, active and reactive power sharing is achieved, ensuring stability at nominal values. The DGs can effectively maintain a constant power profile at desired values, even in the presence of static and dynamic loads.

**Keywords**—Droop control technique, Frequency and voltage stability, Microgrid, Multi-DC bus-based inverter.

## 1. INTRODUCTION

The increased steady electricity demand around the world calls for increased generation, but the challenge facing generation and marketing service companies allowed the appearance and the growth of distribution generators (DGs) techniques. In conjunction with the DGs, the concept of microgrids appeared, adding a new set of benefits that were not possible with the radial power system [1]. The conventional power system is facing the problems of depletion of fossil fuel resources, poor energy efficiency, and environmental pollution [2]. The microgrid is presented in both types of power systems AC and DC, which are installed near the center of load and reduce line losses, increasing reliability and power quality [3]. Many researchers have defined the structure of a microgrid, which is a small-scale power system, including low voltage distribution line, distributed energy resources (DERs) such as renewable energy sources (PV cell, wind turbine), energy storage system (ESS), and microturbine, diesel generator, combined heat and power (CHP) system, power conversion devices, controllable loads, monitoring, and protection devices [4, 5]. The microgrid can operate automatically, this system is capable of self-control and self-management [6]. Furthermore, having the ability to manage energy effectively is one of the advantages of the microgrid;

energy balance and optimization are efficiently maintained within the system, and users are provided with high-quality power as well as increasing the penetration of renewable energy [7]. The most significant concept is that the microgrid should have the ability to operate in both connected mode and island mode. As a result, the microgrid keeps running even though an unexpected disconnection occurs between the microgrid and utility by point of common coupling (PCC) [8, 9]. However, microgrids in islanded mode face voltage and frequency deviation challenges due to DERs' lack of inertia response [9]. Also, with the widespread use of distributed energy resources (DERs) that are replacing synchronous generators (SGs), large-scale power systems are changing rapidly [8], and a sudden loss of power generation units or an increase in a load more than power generation has occurred [3]. As for microgrids operating in connected and island modes, the connected mode allows the utility grid to cover the power shortage, and the surplus power generated in the microgrid can be traded. Furthermore, when the microgrid is in the islanded mode, it is necessary to maintain both the frequency and voltage of the system while also providing the required active and reactive power to loads [6]. Droop control is one of the common methods for microgrid operation in islanded mode, which has the advantage to work without communication signals [10, 11]. A major reason for using droop control in island microgrids is the qualified behavior of droop control with parallel connected inverters, which makes the system highly reliable and typical [12, 13]. A droop control system is useful when used in conjunction with two or more inverters. In common practice, the output power is detected as a feedback factor to compare it with nominal power, with the deviation of DERs voltage controlled according to the proportionality of output power [14–16].

This paper simulates an AC islanding microgrid model, which relies heavily on multiple DC sources as inputs to inverters, which are referred to as DGs in the model. To feed the load, each DG uses a droop control technique to share active and reactive

Received: 09 Feb. 2023

Revised: 04 Jun. 2023

Accepted: 08 Jun. 2023

Available online from 06 Jul. 2023

\*Corresponding author:

E-mail: a.saffarian@scu.ac.ir (A. Saffarian)

DOI: 10.22098/joape.2023.12322.1925

This work is licensed under a [Creative Commons Attribution-NonCommercial 4.0 International License](https://creativecommons.org/licenses/by-nc/4.0/).

Copyright © 2025 University of Mohaghegh Ardabili.

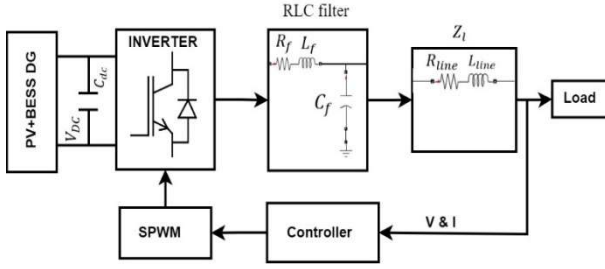


Fig. 1. Block Diagram of DG Based-Inverter

power. With the characteristics of droop control, the DGs supply power to the microgrid based on their capacity. The Droop control will mimic the synchronous generators to stabilize the frequency and voltage despite the constant and dynamic loads. The rest of this paper is arranged as follows; section II briefly describes the system of DG-based-inverter and the concept of droop control. In section III Parallel-connected inverters to an islanded microgrid have been explained. Section IV simulation results and analysis in MATLAB/Simulink software and the results presented including the most important state variables and parameters. Finally, section VI Conclusion discusses the results obtained from the autonomous operation of a multi-DC bus-based inverter.

Overall, the paper contributes to the understanding and implementation of droop control techniques for addressing the frequency and voltage stability challenges in islanded microgrids. It provides simulation-based evidence of the effectiveness of the proposed approach and highlights the advantages of microgrids in terms of reliability, energy efficiency, and the integration of renewable energy sources.

## 2. SYSTEM OF DG BASED-INVERTER

The purpose of this section is to clarify and explain the details of the modelling of DG-based inverters and parallel-connected inverters for the islanded microgrid.

### 2.1. Model of single-phase inverter

The single-phase inverter is an electronic circuit, which converts DC input supply voltage to a symmetrical AC outputs voltage of desired magnitude and frequency [17, 18]. Typically, it consists of a DC power source, and a bridge-type inverter with an RLC filter as shown in Fig. 1. The sinusoidal-PWM (SPWM) is the common technique used in the inverter to produce the specified AC output voltage waveform [19]. The  $R_f$ ,  $L_f$ , and  $C_f$  refer to the resistance, inductance, and capacitance respectively. The line impedance represented by R-line and L-line between the inverter and the load is the equivalent impedance of the connection line or cable. Generally, voltage-source inverters (VSI) are divided into three common categories: Pulse-width Modulated (PWM) Inverters, Square-wave Inverters, and Single-phase Inverters with Voltage Cancellation. Pulse-width modulation inverters take in a constant dc voltage [19, 20].

### 2.2. Concept of droop control

The imbalance in P-F and Q-V will be discussed in this paper based on the execution of the conventional power frequency droop method discussed in [20, 21]. The generally accepted form of the P-F and Q-V droop equations are:

$$\omega - \omega_0 = -m_p(P - P_0) \quad (1)$$

$$V - V_0 = -m_q(Q - Q_0) \quad (2)$$

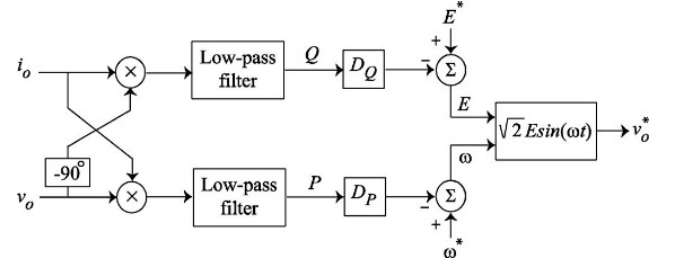


Fig. 2. Conventional droop method [22]

where  $\omega$  and  $\omega_0$  are the output and the nominal frequency respectively. In addition,  $m_p$  is the active power droop coefficient and  $P$  is the inverter active power output. While  $P_0$  represents the nominal power at  $\omega_0$ ,  $V$  and  $V_0$  is the measured output voltage and the nominal voltage respectively,  $m_q$  represents the reactive power droop coefficient,  $Q$  represents the reactive power output, and finally, the  $Q_0$  is the nominal reactive power at  $V_0$ .

Each DG unit will be subject to these equations, slowly changing the values of  $\omega$  and  $V$  in the system, and the amount of active power  $P$  and reactive power  $Q$  supplied by each inverter depends on the values of the  $m_p$  and  $m_q$  coefficients. In conventional control schemes [21], output voltage adjustment is achieved by implementing a proportional-integral (PI) loop that takes into account both the control scheme's system voltage and Q-V droop requirements according to an error equation:

$$V_{err} = V_0 - Vm_q(Q - Q_0) \quad (3)$$

Power sharing is controlled by changing the relative droop gradient ( $m_p/m_q$ ) and the power set point ( $P_0/Q_0$ ) of each inverter. Changes in  $m_p$  and/or  $m_q$  are implemented by the entire system controller, which dynamically adjusts the set points of the DG unit in the microgrid [20].

In addition, the characteristic techniques droop control method has also been referred to as independent, autonomous, and wireless control because intercommunication links between converters have been eliminated.

Conventional active power control (frequency droop characteristic) and reactive power control (voltage droop characteristic) are illustrated in Fig. 2 [22].

The principles of the conventional droop methods can be explained by considering an equivalent circuit of a voltage source converter (VSC) connected to an AC bus, as shown in Fig. 3. If switching ripples and high-frequency harmonics are neglected, the VSC can be modelled as an AC source, with the voltage of  $E\angle\delta$ . In addition, assume that the common AC bus voltage is  $V_{com}$  and the converter output impedance and the line impedance are lumped as a single effective line impedance of  $Z\angle\theta$ . The complex power supplied to the AC common bus is calculated by the following formula.

$$S = V_{com}I^* = \frac{V_{com}E\angle\theta - \delta}{Z} - \frac{V_{com}^2\angle\theta}{Z} \quad (4)$$

from which the real and reactive powers are achieved as the bellow

$$\begin{cases} P = \frac{V_{com}E}{Z} \cos(\theta - \delta) - \frac{V_{com}^2}{Z} \cos(\theta) \\ Q = \frac{V_{com}E}{Z} \sin(\theta - \delta) - \frac{V_{com}^2}{Z} \sin(\theta) \end{cases} \quad (5)$$

If the effective line impedance,  $Z\angle\theta$ , is assumed to be purely inductive,  $\theta = 90^\circ$ , then (5) can be reduced to

$$\begin{cases} P = \frac{V_{com}E}{Z} \sin\delta \\ Q = \frac{V_{com}E \cos\delta}{Z} - \frac{V_{com}^2}{Z} \end{cases} \quad (6)$$

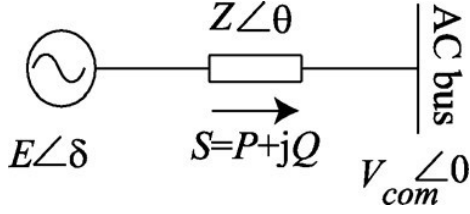


Fig. 3. Simplified diagram of a converter connected to the microgrid [22]

If the phase angle ( $\delta$ ) difference between the converter output voltage and the common AC bus,  $\delta$ , is small enough, then,  $\sin \delta \approx \delta$  and  $\cos \delta \approx 1$ .

Thus, one can apply the frequency and voltage droop characteristics to fine-tune the voltage reference of the VSC [23, 24], as shown in Fig. 2 based on

$$\begin{cases} \omega = \omega_0 - m_P P \\ V = V_0 - m_Q Q \end{cases} \quad (7)$$

In the former approach,  $m_P$  and  $m_Q$ , are determined based on the converter power rating and the maximum allowable voltage and frequency deviations. For instance, in a microgrid with DERs, corresponding should satisfy the following constraints [25].

$$\begin{cases} m_{P1} P_{n1} = m_{P2} P_{n2} = \dots = m_{PN} P_{nN} = \Delta\omega_{max} \\ m_{q1} Q_{n1} = m_{q2} Q_{n2} = \dots = m_{qN} Q_{nN} = \Delta V_{max} \end{cases} \quad (8)$$

Where  $\Delta\omega_{max}$  and  $\Delta V_{max}$  are the maximum allowable angular frequency and voltage deviations, respectively.  $P_{ni}$  and  $Q_{ni}$  are the nominal active and reactive power of the  $i$ th DER. During the grid-tied operation of the microgrid, the DER voltage and angular frequency,  $V$  and  $\omega$ , are enforced by the grid. The DER output active and reactive power references,  $P^{ref}$  and  $Q^{ref}$ , can hence be adjusted through  $V_0$  and  $\omega_0$  [26] as

$$\begin{cases} P^{ref} = \frac{\omega_0 - \omega}{m_P} \\ Q^{ref} = \frac{V_0 - V}{m_Q} \end{cases} \quad (9)$$

The dynamics response of the conventional primary control, on the simplified system of Fig. 3, can be studied by linearizing (6) and (7).

### 3. PARALLEL-CONNECTED INVERTERS TO AN ISLANDED MICROGRID

As shown in Fig. 4, parallel connected inverters are used to supply power to the islanded microgrid. The power platform consists of different types of DC power resources such as PV panels, batteries, and DC wind turbines as the input power to the inverter. The parallel-connected inverter will operate by applying the droop control method as an essential method to balance the power according to load change. In addition, Fig. 4 shows the characteristics of the inverter control, which includes droop control block, voltage control block, and SPWM block.

Previously, a conventional PI controller is used with the voltage feedback loop to regulate the output voltage [27]. The active and reactive power of each inverter is obtained based on the voltage and current measurements after filtering later and supplied to the proposed controller with a new value for reference voltage,  $V_{ref}$ , and angular frequency,  $\omega_i$  which will be led to proportional power sharing [20, 22].

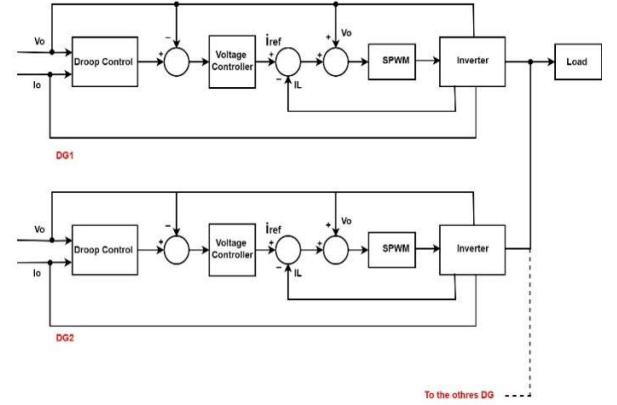


Fig. 4. Configuration of parallel inverter-based islanded microgrid

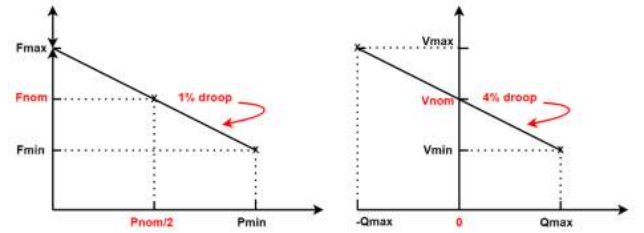


Fig. 5. The droop characteristics of the inverter control

## 4. SIMULATION RESULTS AND ANALYSIS

In this simulation, droop control is commonly used as the speed control mode of the governor of a prime mover driving a synchronous generator connected to an electrical grid. The droop characteristics of the inverter control is shown in Fig. 5.

As in Fig. 5 the droops P/F & Q/V are illustrated below:

- The droop P/F is set to 1% of the nominal frequency of 50 Hz, meaning that microgrid frequency is allowed to vary from 50.5 Hz (inverter produces no active power) to 49.5 Hz (inverter produces its nominal active power).
- The droop Q/V is set to 4% of the nominal voltage of 600 V, meaning that the microgrid voltage at the PCC bus is allowed to vary from 612 Vrms (inverter produces its full inductive power) to 588 Vrms (inverter produces its full capacitive power).

In Fig. 6 the MATLAB/Simulink model presents the DGs-based parallel inverters as a microgrid in islanded mode. The microgrid consists of two parallel inverters subsystems DG units, with power ratings of 600 kVA, and 400 kVA with a nominal frequency of

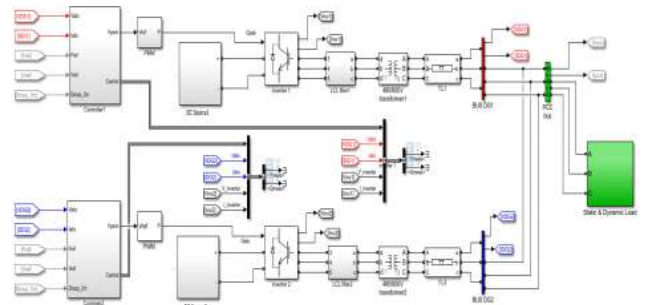


Fig. 6. DG-based Parallel inverters

Table 1. The parameters of the microgrid model

	DG	Constant Load	Dynamic Load
Nominal power S1	600 kVA	Load1 450 kW / 100 kVAr	350 kW
Nominal power S2	400 kVA	Load2 75 kW / 0 kVAr	100 kVAr
Frequency	50 Hz		

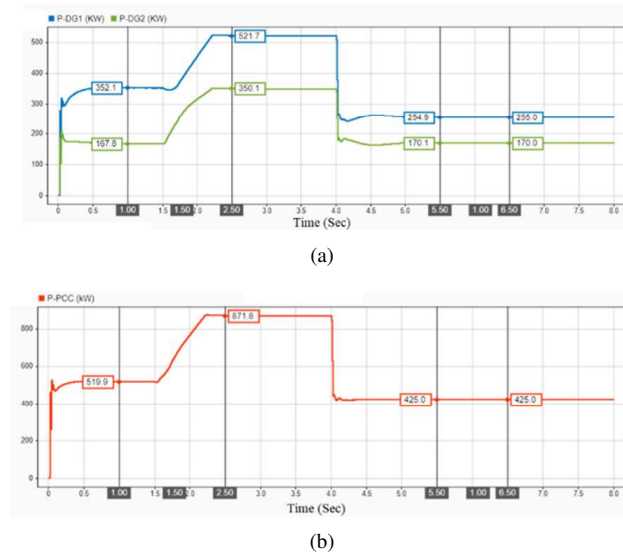


Fig. 7. Active power reference of load, (a) is the active power of DG, DG2, and (b) is the total power produced at PCC.

50 Hz. The inverters are connected to the islanded microgrid with constant active and reactive power loads. Furthermore, the dynamic load model is used to change the microgrid load dynamically. Each subsystem also includes a control system and an SPWM generator feeding inverter. The parameters of the microgrid model are as shown in Table 1, the total power load is 875 kW as the active power w the reactive power load is 200 kVAr.

As a result, the active droop coefficient of the converter followed the load demand. Fig. 7 shows the reference demand of load active power of the first and the second converter. The output active power of the converters is shared between two DG units to cover the load demand at PCC. From the operation starting until 1.5s, there is a change through the reference active power from 0-519.9kW which is shared between DG1 and DG2 with the rated 352.1kW and 167.8k respectively. At the time 1.5s the load is raised to reach to maximum tip at 875.1.8kW, after 4s about 350kW of the power load is disconcerted from the grid, and this action leads to the fall of the total load to stay at 425kW. The relative between active power and frequency is illustrated in Fig. 8.

The DGs are sharing the total active power via the converters depending on the rated capacity. The frequency decreases with the increase of the active power of the load and verse versa. The frequency should be stable even with the change of the active power to keep the grid in running mode.

In Fig. 8, the grid is working without control until 1.5s that's why the frequency is having a deviation and increased to 50.29-50.25Hz with active power close to 515kW. On the 1.5s the grid is working with the control, although the power is increased to 541.6 kW the frequency reads 49.99Hz during a short time (0.09s). Even with the maximum power load of about 875kW between the time 2.2s-4s, the frequency stays at the steady state values. After 4s, about 350kW of the load is removed from the grid which leads to raised frequency a bit (50.13Hz), then the actual frequency is optimized by the reference frequency to keep

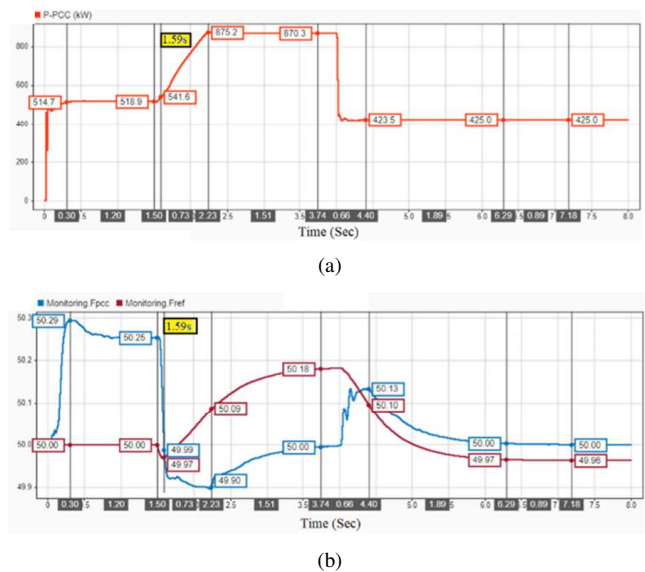


Fig. 8. The relevance between active power and frequency, (a) the active power at PCC, (b) the frequency at the PCC in blue colour, and the reference frequency in brown colour.

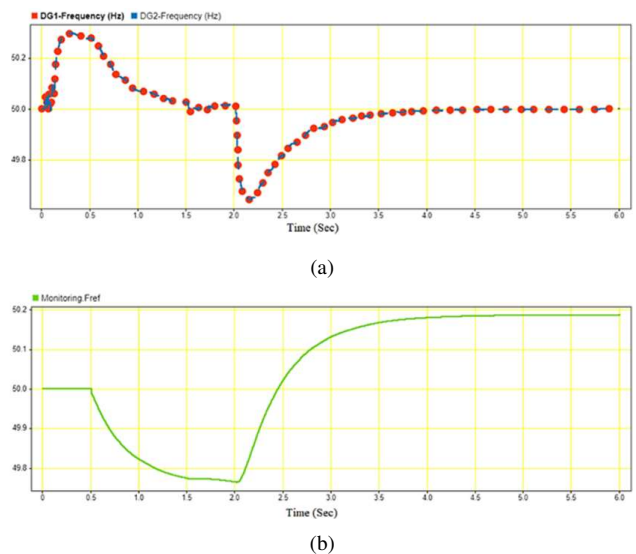


Fig. 9. Frequency of DG1, DG2, and the reference frequency, (a) the frequency curve for both DGs, red balls curve, and blue lines curve represent the frequency behaviours for DG1 and DG2 respectively, and (b) is the references frequency of the system.

it at the nominal value of 50Hz in the limited time. Even though the coefficients of the droop are different, it affects the output active power of the DGs converters and both local frequencies are changing together; so always the system has the same frequency (see Fig. 9). The control system follows the reference frequency; hence the reference frequency given by the droop control is the same as the actual measured frequency of the system.

The behaviors of reactive power are somewhat close to the behaviors of active power in terms of sharing productive capacity see Figs. 7 and 10. Both generators' dispositions to participate in the productive capacity (power sharing) depend on the droop technique as a result of the load imposed on the microgrid.

The reactive power is shown in Fig. 10, the reactive power at PCC is raised to read about 98 kVAr until 105s. The power was



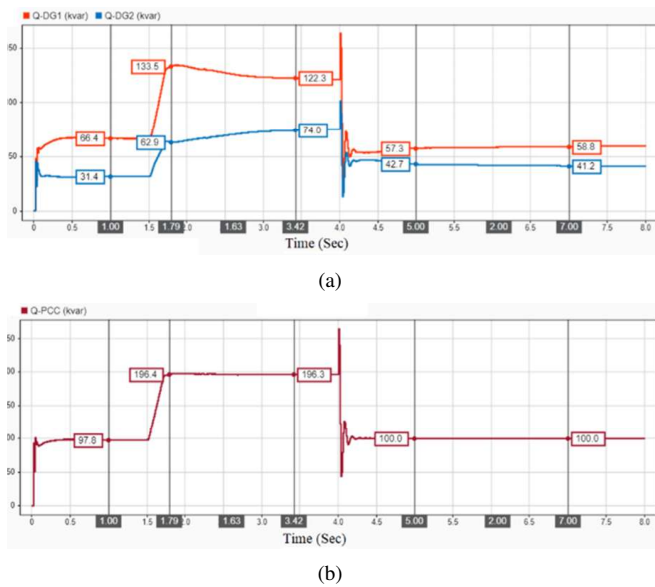


Fig. 10. Reactive power reference of DGs and load, (a) is the reactive power of DG1 and DG2 (b) is the total reactive power load at PCC.

divided between the DGs, 68% for the first DG1 and 32% for the second. Between 1.5s-1.79s, the reactive power load increases to reach more than 196 kVar and continues until the fourth second. At the same time, in the fourth second, the energy is disturbed for 0.2 seconds to record a value of 43-264 kVar due to disconnecting part of the load and then continues with a value of 100 kVar, which is shared into DGs with the rate values close to 60% to 40%.

However, there is a fundamental difference between the active and reactive power on the stability of frequency and voltage. Fig. 8 illustrates the relationship between the effects of active power and frequency. Next, Fig. 11 will demonstrate the impact of reactive power on voltage.

Fig. 11 shows, the sharp drop in the voltage (340 V) of the PCC at 0.04s and 100.5 kVar, which is due to the starting operation of the load and the effects of the reactive power load. the voltage is returned shortly to the comparable nominal value to be stable at the voltage (601 V) and the reactive power load is close to 98 kVar until 1.5s. Although the reactive power is increased to twice (188 kVar) at 1.7s, the voltage deviation is 2% only then returning to the close nominal value in less than 1s.

The voltage remains stable until the seconds fourth due to voltage control and limited changes in the reactive power load. Due to the removal of a part of the load the reactive power falls to 50%, causing an increase in the voltage by around 3% for a short time, less than 0.3s. However, the voltage stays stable at the nominal value (600V). on the other hand, the reactive power stays constant at (100 kVar).

## 5. CONCLUSION

This paper studied the autonomous dynamic operation of DG-based multi-converters by using two sources in parallel as a microgrid in islanded mode. MATLAB/Simulink was used to simulate the model of droop control to mimic the microgrid. Droop control of frequency and voltage is applied to face the active and reactive power of the output converter. Through the results, both converters are shared the total power (active and reactive power) with the change of the load depending on the capacity of each DG and the droop coefficients. In addition, the frequency and voltage were stable at the acceptable scale by reducing the disturbances, this is an indication of the success and effectiveness of the droop control system.

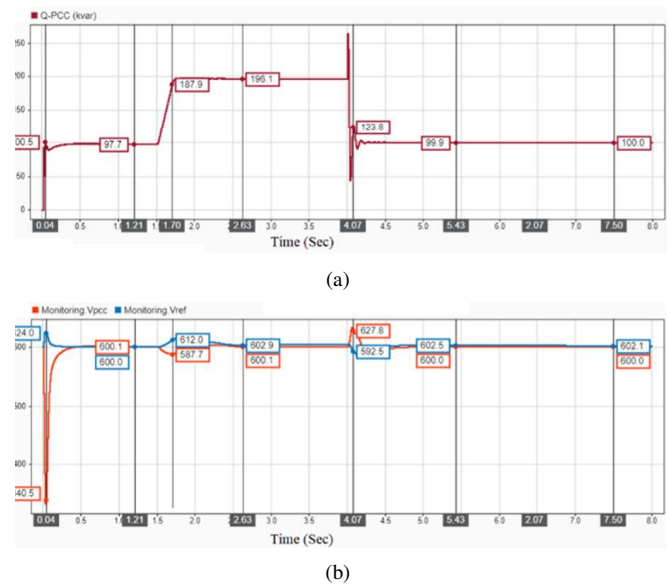


Fig. 11. The relation of reactive power with voltage stability, (a) reactive power load at PCC, (b) voltage profile at PCC, the actual voltage at PCC (red line), and the reference voltage (blue line).

## Acknowledgement

Thankful for the JOAPE journal editorial board for their work on the original version of this paper.

## REFERENCES

- [1] K. Twaisan and N. Barişçi, "Integrated distributed energy resources (der) and microgrids: Modeling and optimization of ders," *Electronics*, vol. 11, no. 18, p. 2816, 2022.
- [2] M. Mohebbi-Gharavanlou, S. Nojavan, and K. Zareh, "Energy management of virtual power plant to participate in the electricity market using robust optimization," *J. Oper. Autom. Power Eng.*, vol. 8, no. 1, pp. 43–56, 2020.
- [3] S. Ali, Z. Zheng, M. Aillerie, J.-P. Sawicki, M.-C. Pera, and D. Hissel, "A review of dc microgrid energy management systems dedicated to residential applications," *Energies*, vol. 14, no. 14, p. 4308, 2021.
- [4] R. Khan, N. Islam, S.K. Das, S. Muyeen, S.I. Moyeen, M.F. Ali, Z. Tasneem, M.R. Islam, D.K. Saha, M.F.R. Badal, *et al.*, "Energy sustainability—survey on technology and control of microgrid, smart grid and virtual power plant," *IEEE Access*, vol. 9, pp. 104663–104694, 2021.
- [5] P. Venkata, V. Pandya, and A. Sant, "Data mining model based differential microgrid fault classification using svm considering voltage and current distortions," *J. Oper. Autom. Power Eng.*, vol. 11, no. 3, pp. 162–172, 2023.
- [6] A. Fathi, Q. Shafiee, and H. Bevrani, "Robust frequency control of microgrids using an extended virtual synchronous generator," *IEEE Trans. Power Syst.*, vol. 33, no. 6, pp. 6289–6297, 2018.
- [7] K.Y. Yap, C.R. Sarimuthu, and J.M.-Y. Lim, "Virtual inertia-based inverters for mitigating frequency instability in grid-connected renewable energy system: A review," *Appl. Sci.*, vol. 9, no. 24, p. 5300, 2019.
- [8] T. Madiba, R. Bansal, N. Mbungu, M. Bettayeb, R. Naidoo, and M. Siti, "Under-frequency load shedding of microgrid systems: a review," *Int. J. Model. Simul.*, vol. 42, no. 4, pp. 653–679, 2022.
- [9] J. Singh, S. Prakash Singh, K. Shanker Verma, A. Iqbal, and B. Kumar, "Recent control techniques and management of ac microgrids: A critical review on issues, strategies, and future

- trends,” *Int. Trans. Electr. Energy Syst.*, vol. 31, no. 11, p. e13035, 2021.
- [10] Q.-C. Zhong, “Robust droop controller for accurate proportional load sharing among inverters operated in parallel,” *IEEE Trans. Ind. Electron.*, vol. 60, no. 4, pp. 1281–1290, 2011.
- [11] Y. Sun, X. Hou, J. Yang, H. Han, M. Su, and J.M. Guerrero, “New perspectives on droop control in ac microgrid,” *IEEE Trans. Ind. Electron.*, vol. 64, no. 7, pp. 5741–5745, 2017.
- [12] A.M. Bouzid, J.M. Guerrero, A. Cheriti, M. Bouhamida, P. Sicard, and M. Benghanem, “A survey on control of electric power distributed generation systems for microgrid applications,” *Renew. Sustain. Energy Rev.*, vol. 44, pp. 751–766, 2015.
- [13] D.G. Photovoltaics and E. Storage, “Ieee guide for design, operation, and integration of distributed resource island systems with electric power systems,” 2011.
- [14] S. Alghamdi, H.F. Sindi, A. Al-Durra, A.A. Alhussainy, M. Rawa, H. Kotb, and K.M. AboRas, “Reduction in voltage harmonics of parallel inverters based on robust droop controller in islanded microgrid,” *Mathematics*, vol. 11, no. 1, p. 172, 2023.
- [15] P. Ilyushin, V. Volnyi, K. Suslov, and S. Filippov, “State-of-the-art literature review of power flow control methods for low-voltage ac and ac-dc microgrids,” *Energies*, vol. 16, no. 7, p. 3153, 2023.
- [16] S. Bruno, G. Giannoccaro, C. Iurlaro, M. La Scala, and C. Rodio, “Power hardware-in-the-loop test of a low-cost synthetic inertia controller for battery energy storage system,” *Energies*, vol. 15, no. 9, p. 3016, 2022.
- [17] Y. Zhou, L. Liu, H. Li, and L. Wang, “Real time digital simulation (rtds) of a novel battery-integrated pv system for high penetration application,” in *The 2nd IEEE Int. Symp. Power Electron. Gener.*, pp. 786–790, IEEE, 2010.
- [18] J.C. Vasquez, J.M. Guerrero, M. Savaghebi, J. Eloy-Garcia, and R. Teodorescu, “Modeling, analysis, and design of stationary-reference-frame droop-controlled parallel three-phase voltage source inverters,” *IEEE Trans. Ind. Electron.*, vol. 60, no. 4, pp. 1271–1280, 2012.
- [19] A. Khajezadeh, M. Amirinejad, and S. Rafieisarbejan, “An introduction to inverters and applications for system design and control wave power,” *Int. J. Sci. Eng. Res.*, vol. 5, no. 7, 2014.
- [20] M.B. Cheema, S.A. Hasnain, M.M. Ahsan, M. Umer, and G. Ahmad, “Comparative analysis of spwm and square wave output filtration based pure sine wave inverters,” in *2015 IEEE 15th International Conference on Environment and Electrical Engineering (EEEIC)*, pp. 38–42, IEEE, 2015.
- [21] J.M. Guerrero, J.C. Vasquez, J. Matas, L.G. De Vicuña, and M. Castilla, “Hierarchical control of droop-controlled ac and dc microgrids—a general approach toward standardization,” *IEEE Trans. Ind. Electron.*, vol. 58, no. 1, pp. 158–172, 2010.
- [22] A. Bidram and A. Davoudi, “Hierarchical structure of microgrids control system,” *IEEE Trans. Smart Grid*, vol. 3, no. 4, pp. 1963–1976, 2012.
- [23] J.M. Guerrero, L. Hang, and J. Uceda, “Control of distributed uninterruptible power supply systems,” *IEEE Trans. Ind. Electron.*, vol. 55, no. 8, pp. 2845–2859, 2008.
- [24] J.M. Guerrero, J.C. Vasquez, J. Matas, M. Castilla, and L.G. de Vicuña, “Control strategy for flexible microgrid based on parallel line-interactive ups systems,” *IEEE Trans. Ind. Electron.*, vol. 56, no. 3, pp. 726–736, 2008.
- [25] E. Rokrok and M.E.H. Golshan, “Adaptive voltage droop scheme for voltage source converters in an islanded multibus microgrid,” *IET Gener. Transm. Distrib.*, vol. 4, no. 5, pp. 562–578, 2010.
- [26] J.P. Lopes, C.L. Moreira, and A. Madureira, “Defining control strategies for microgrids islanded operation,” *IEEE Trans. Power Syst.*, vol. 21, no. 2, pp. 916–924, 2006.
- [27] P. Monica, M. Kowsalya, and P. Tejaswi, “Load sharing control of parallel operated single phase inverters,” *Energy procedia*, vol. 117, pp. 600–606, 2017.